# Functional Approach to Microwave Postproduction Tuning

JOHN W. BANDLER, FELLOW, IEEE, AND ALY E. SALAMA, MEMBER, IEEE

*Abstract* — **This paper deals with the postproduction tuning problem in microwave circuits using the functional approach. The main aspects of the problem are addressed. In particular, we consider the choice of the critical samples of the response, the choice of the most effective tunable parameters, and the description of two functional tuning algorithms. Minimax optimization is used to identify the tuning frequencies, and least-one optimization is employed to minimize the number of tunable parameters. Worst-case analysis is utilized to reduce the size of the problem. The different concepts, definitions, and techniques are illustrated on a simple two-section transformer example. Recent, well-documented, and highly efficient optimization packages are utilized to implement the least-one and minimax optimization problems.**

## I. Introduction

POSTPRODUCTION TUNING is often essential in the manufacturing of electrical circuits. Tolerances on the circuit components, parasitic effects, and uncertainties in the circuit model cause deviations in the manufactured circuit performance, and violation of the design specifications may result. Therefore, postproduction tuning is included in the final stages of the production process to readjust the network performance in an effort to meet the specifications.

Tuning has formally been considered as an integral part of the design process [1], the objective being to relax the tolerances and compensate for the uncertainties in the model parameters. We give here a unified and integrated approach to the postproduction tuning problem. Minimax optimization is used in the nominal design stage to provide us with the critical frequencies. Therefore, the tuning frequencies are identified. The least-one optimization is used to minimize the number of tunable parameters needed to tune all possible outcomes of a manufactured circuit. Worst-case analysis is employed to reduce the size of the problem. Two functional tuning algorithms are presented. Both algorithms are based on measuring the response of the circuit at a number of critical frequencies and formulating the postproduction tuning problem as an optimization problem, which is solved on-line for the required changes in the tunable parameter values.

A two-section transformer example is utilized to illustrate the different concepts, definitions, and techniques. Recent, well-documented, well-tested, and highly efficient optimization packages are utilized to implement the different proposed optimization problems.

Manuscript received July 13, 1984; revised November 27, 1984 This work was supported in part by the Natural Sciences and Engineering Research Council of Canada under Grant A7239. This paper is based on material presented at the 1983 IEEE International Microwave Symposium, Boston, MA, June 1–3, 1983.

J. W. Bandler is with the Simulation Optimization Systems Research Laboratory and the Department of Electrical and Computer Engineering, McMaster University, Hamilton, Canada L8S 4L7. He is also with Optimization Systems Associates, 163 Watson's Lane, Dundas, Ontario, Canada L9H 6L1.

A. E Salama was with the Simulation Optimization Systems Research Laboratory and the Department of Electrical and Computer Engineering, McMaster University, Hamilton, Canada L8S 4L7. He is now with the Department of Electronics and Electrical Communications Engineering, Cairo University, Giza, Egypt

## II. Fundamental Concepts and Definitions

To illustrate the various definitions and results in this paper, we consider a simple example, a two-section 10:1 quarter-wave transformer, shown in Fig. 1.

The design parameters are the normalized characteristic impedances of the two sections, namely $Z_1$ and $Z_2$. Let their nominal values be given by

$$\boldsymbol{\phi}^0 = \begin{bmatrix} \phi_1^0 \\ \phi_2^0 \end{bmatrix} = \begin{bmatrix} Z_1^0 \\ Z_2^0 \end{bmatrix} = \begin{bmatrix} 2.2361 \\ 4.4721 \end{bmatrix}$$

where superscript 0 refers to the nominal values. Due to manufacturing tolerances, the actual values of the circuit parameters are, in general, different from nominal and can be expressed as

$$\boldsymbol{\phi} = \begin{bmatrix} \phi_1 \\ \phi_2 \end{bmatrix} = \begin{bmatrix} Z_1 \\ Z_2 \end{bmatrix} = \begin{bmatrix} Z_1^0 \\ Z_2^0 \end{bmatrix} + \begin{bmatrix} \epsilon_{Z_1} & 0 \\ 0 & \epsilon_{Z_2} \end{bmatrix} \begin{bmatrix} \mu_{Z_1} \\ \mu_{Z_2} \end{bmatrix}$$

where $\epsilon_{Z_1}$ and $\epsilon_{Z_2}$ are the tolerances associated with $Z_1$ and $Z_2$, respectively. $\mu_{Z_1}$ and $\mu_{Z_2}$ are multipliers constrained between $-1.0$ and 1.0.

Similarly, the actual parameter values of a $n_\phi$-parameter circuit can be expressed as

$$\boldsymbol{\phi} \triangleq \boldsymbol{\phi}^0 + \boldsymbol{E}\boldsymbol{\mu} \tag{1a}$$

where

$$\boldsymbol{\phi}^0 \triangleq \left[\phi_1^0 \phi_2^0 \cdots \phi_{n_\phi}^0\right]^T \tag{1b}$$

$$\boldsymbol{E} \triangleq \operatorname{diag}\{\epsilon_1, \epsilon_2, \cdots, \epsilon_{n_\phi}\} \tag{1c}$$

$$-1 \leq \mu_i \leq 1, \qquad i \in I_\phi \tag{1d}$$

and

$$I_\phi \triangleq \{1, 2, \cdots, n_\phi\}. \tag{1e}$$

$\boldsymbol{\phi}^0$ is the nominal vector and $\epsilon_i$ is the tolerance associated with the $i$th element $\phi_i$ [1], [2]. Therefore, in the context of

0018-9480/85/0400-0302$01.00 ©1985 IEEE

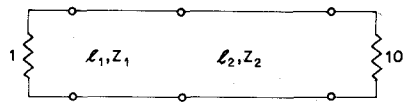


Fig. 1. The two-section 10:1 quarter-wave transformer.

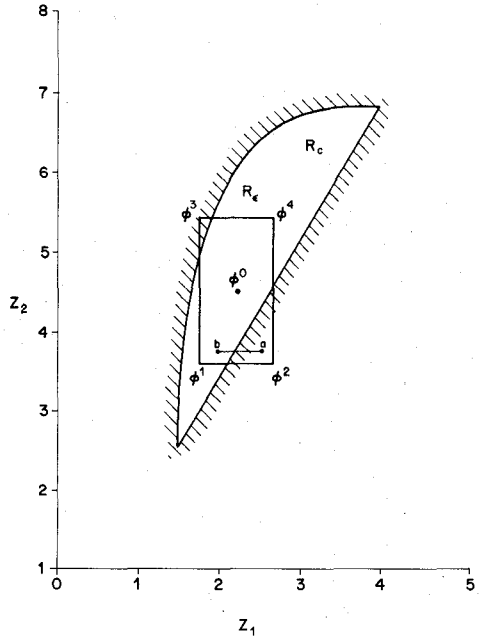


Fig. 2. Illustration of the two-section transformer tolerance region and feasible region in the parameter space of $Z_1$ and $Z_2$.

the two-section transformer example, we could have considered other design parameters, e.g., $l_1$ and $l_2$ or any other effects.

The designer has no control over $\mu$, and this leads to the concept of the tolerance region $R_\epsilon$ defined by

$$R_\epsilon \triangleq \left\{ \phi | \phi_i = \phi_i^0 + \epsilon_i \mu_i,\ -1 \leq \mu_i \leq 1,\ i \in I_\phi \right\} \tag{2}$$

which is a convex regular polytope of $n_\phi$ dimensions with sides of length $2\epsilon_i$, $i \in I_\phi$.

The tolerance region of the two parameters $Z_1$ and $Z_2$ of the two-section transformer is shown in Fig. 2 with $\epsilon_{Z_1}/Z_1^0 = \epsilon_{Z_2}/Z_2^0 = 0.2$. Note that it is a rectangular region.

The extreme points of $R_\epsilon$ are defined by setting $\mu_i = \pm 1$. Thus, the set of vertices may be defined by

$$R_v \triangleq \left\{ \phi | \phi_i = \phi_i^0 + \epsilon_i \mu_i,\ \mu_i \in \{-1,1\},\ i \in I_\phi \right\}. \tag{3}$$

The number of points in $R_v$ is $2^{n_\phi}$. For the tolerance region of Fig. 2, we have four vertices. A vertex number is given according to the formula

$$r \triangleq 1 + \sum_{i=1}^{n_\phi} \left[ \frac{\mu_i^r + 1}{2} \right] 2^{i-1} \tag{4a}$$

$$\mu_i^r \in \{-1,1\},\ i \in I_\phi. \tag{4b}$$

Consequently, the $r$th vertex is referred to by $\phi^r$, and an index set of all these vertices is defined as

$$I_v \triangleq \{1,2,\cdots,2^{n_\phi}\}. \tag{5}$$

In Fig. 2, the four vertices are shown numbered according to (4a).

In a typical design problem, the output response of a circuit $F(\phi, \omega)$ is required to meet design specification $S(\omega)$ at a number of discrete frequency points $\omega_i$. Therefore, a number of inequality constraints given by

$$f_i(\phi) \triangleq w_i(F(\phi, \omega_i) - S(\omega_i)) \leq 0, \qquad i \in I_c \tag{6a}$$

where

$$I_c \triangleq \{1,2,\cdots,m\} \tag{6b}$$

should be satisfied [3]. $w_i$ is a weighting function that is positive or negative according to whether $S(\omega_i)$ is an upper or lower specification, respectively. Constraints (6a) define a region in the parameter space. This region is usually referred to as the feasible region and is defined as

$$R_c \triangleq \{ \phi | f_i(\phi) \leq 0,\ i \in I_c \}. \tag{7}$$

For the two-section transformer, it is required that the absolute value of the reflection coefficient over the frequency band of interest, 0.5–1.5 GHz, should not exceed 0.55. Therefore, $F(\phi, \omega)$ is the absolute value of the reflection coefficient and $S(\omega) = 0.55$. Eleven sample points are taken over the range of interest, namely $0.5, 0.6, \cdots, 1.5$ GHz. Consequently, $I_c = \{1,2,\cdots,11\}$. The feasible region $R_c$ corresponding to constraints (6a) with $w_i = 1.0$, $i \in I_c$ is shown in Fig. 2.

For $\pm 20$-percent tolerances on the characteristic impedances $Z_1$ and $Z_2$, not all the tolerance region outcomes are included in the feasible region $R_c$. To tune all possible outcomes of a manufactured product to design specifications, a subset of the circuit parameters is needed to be readjusted for postproduction tuning. Therefore, we have to know at the design stage this subset of minimum cardinality such that all possible outcomes of the tolerance region are tunable to satisfy the design specifications. This is usually referred to as the *tuning parameter selection problem*.

This subset $I_t^*$ of tunable parameters of cardinality $k$ is usually chosen from a larger subset $I_t \subseteq I_\phi$ of all possible tunable parameter candidates. The tunable parameter candidates are those parameters that can be adjusted after manufacturing.

For the two-section transformer, let us assume that the subset $I_t$ corresponds to parameters $Z_1$ and $Z_2$. Accordingly, $I_t^*$ will correspond to either one of them or both of them depending on the tuning parameter selection algorithm.

The circuit parameters (1) with tuning taken into consideration are given by

$$\phi_i \triangleq \begin{cases} \phi_i^0 + \mu_i \epsilon_i, & i \notin I_t^* \\ \phi_i^0 + \mu_i \epsilon_i + \rho_i t_i, & i \in I_t^* \end{cases} \qquad i \in I_\phi \tag{8a}$$

where

$$-1 \leq \rho_i \leq 1, \qquad i \in I_t^* \tag{8b}$$

for two-way tuning. In a more compact form, (8a) could be expressed as

$$\phi = \phi^0 + E\mu + T\rho \tag{8c}$$

where

$$\boldsymbol{T} \triangleq \operatorname{diag}\{t_1, t_2, \cdots, t_{n_\phi}\} \tag{8d}$$

and $t_i$ is the tuning amount associated with the $i$th element, $t_i = 0$ if $i \notin I_t^*$.

For the two-section transformer, if we assume that $Z_1$ is the only tunable element, then the circuit parameters can be expressed as follows:

$$\begin{bmatrix}\phi_1\\ \phi_2\end{bmatrix} = \begin{bmatrix}Z_1\\ Z_2\end{bmatrix} = \begin{bmatrix}Z_1^0\\ Z_2^0\end{bmatrix} + \begin{bmatrix}\mu_{Z_1}\epsilon_{Z_1}\\ \mu_{Z_2}\epsilon_{Z_2}\end{bmatrix} + \begin{bmatrix}\rho_{Z_1}t_{Z_1}\\ 0\end{bmatrix}.$$

A tuning algorithm is needed to carry out the required adjustments of the tunable parameters of a manufactured circuit that violates the design specifications. The computer-aided postproduction tuning algorithm automates and at the same time optimally performs the process, i.e., it eliminates the experimental trial-and-error approach. The problem of finding these adjustments is referred to as the *postproduction tuning assignment problem*.

In the context of the two-section transformer example, this means that for a certain production outcome represented by $[\mu_{Z_1}\mu_{Z_2}]^T$, where $T$ indicates the transpose, which is out of the feasible region $R_c$, it is required to find the change in the tunable element $Z_1$ represented by $\rho_{Z_1}$ such that the tuned outcome will be inside the feasible region. A typical example is shown in Fig. 2, where point $a$ represents an untuned outcome and point $b$ represents the outcome after tuning.

## III. Selection of Tuning Frequencies

Over the frequency band of interest, it is required to find a subset of critical frequency points $\omega_i$, $i \in I_c^*$, where $I_c^* \subset I_c$, which is used in selecting the tunable parameters.

The effect of including a particular frequency point is to emphasize the response control at that frequency. Since the response gradients for two closely spaced frequencies will be almost collinear, the frequencies should be reasonably spaced and placed in areas where tight control over the response is desired [4].

We have utilized a minimax design criterion to identify the set of critical frequencies $I_c^*$. In the nominal network design problem, it is required to find the set of parameters $\phi^0$ which optimally satisfies the design constraints. Let

$$M_f(\phi^0) \triangleq \max_{i \in I_c} f_i(\phi^0). \tag{9a}$$

Then, our nominal design problem is to

$$\underset{\phi^0}{\text{minimize}}\, M_f(\phi^0) \tag{9b}$$

which is converted to a regular nonlinear programming problem as follows:

$$\underset{\phi^0, z}{\text{minimize}}\, z \tag{10a}$$

subject to

$$f_i(\phi^0) \leqslant z, \qquad i \in I_c \tag{10b}$$

where $z$ is an independent additional variable.

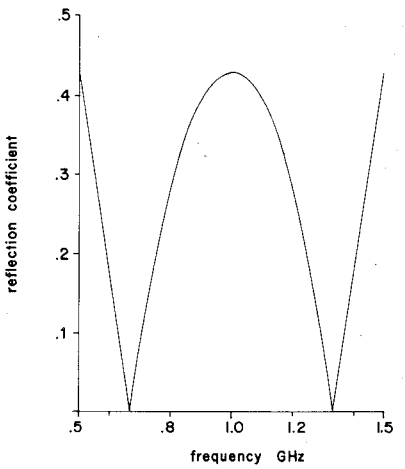


Fig. 3. The minimax response of the two-section transformer.

The solution of the optimization problem (10) provides us with theoretically justifiable critical (or active) functions $f_j(\phi)$, $j \in I_c^*$. The active functions are those approximately equal to $z$ at the solution, i.e., the functions that reach the maximum value at the minimax solution (equiripple response).

For the two-section transformer example, we implemented the minimax problem of (10), with $Z_1^0$ and $Z_2^0$ as the only variables. The resulting minimax response is shown in Fig. 3, which identifies the frequency points 0.5, 1.0, and 1.5 GHz as the three critical frequencies; therefore $I_c^* = \{1, 6, 11\}$. The optimum values of $Z_1^0$ and $Z_2^0$ are 2.2361 and 4.4721, respectively, as we pointed out earlier.

## IV. Selection of Tunable Elements

It is required to find the minimum number of tunable parameters to tune all possible manufactured outcomes of the circuit. A manufactured outcome of the circuit would be a point of the region $R_\epsilon$ (2). Worst-case analysis is carried out to identify the critical points of this region [5]. A worst-case point is assumed to occur at a vertex (5) of $R_\epsilon$. A worst-case algorithm that utilizes first-order sensitivities is employed. The algorithm is similar to the one proposed by Brayton *et al.* [5].

For every critical function $f_i(\phi)$, $i \in I_c^*$, one or more vertices are selected. Let $I_{vi} \subset I_v$ be the index set of the worst-case vertices corresponding to the function $f_i(\phi)$, $i \in I_c^*$, and let

$$I_v^* \triangleq \bigcup_i I_{vi}, \qquad i \in I_c^* \tag{11}$$

define the index set of critical vertices $I_v^* \subset I_v$.

For the two-section transformer example, we have three critical frequencies, 0.5, 1.0, and 1.5 GHz. Vertex number 3 is the worst-case vertex for the 0.5- and 1.5-GHz critical frequencies. Vertex number 2 is the worst-case vertex for the 1.0-GHz critical frequency. In terms of the notation of (11), we have $I_{v1} = \{3\}$, $I_{v6} = \{2\}$, and $I_{v,11} = \{3\}$. Consequently, $I_v^* = \{2, 3\}$.

The subset $I_t^*$ of the tunable parameters are obtained by solving an optimization problem. A least-one objective

function is utilized. In data fitting, the least-one criterion has been extensively applied to eliminate the faulty data. We utilized it here to force as many parameters as possible to have a zero value of $t_i$. This consequently reduces the number of tunable parameters required to tune all worst-case vertices. At the solution, we obtain $I_t^*$ from the set $I_t$ using the following relation:

$$I_t^* \triangleq \{ i | t_i \neq 0,\ i \in I_t \}. \tag{12}$$

The least-one optimization problem is given as follows:

$$\text{minimize} \sum_{i \in I_t} t_i / \phi_i^0 \tag{13a}$$

w.r.t. $t_i$, $\rho_i^r$, $i \in I_t$, $r \in I_v^*$, where

$$t_i \geq 0, \qquad i \in I_t \tag{13b}$$

$$-1 \leq \rho_i^r \leq 1, \qquad i \in I_t,\ r \in I_v^* \tag{13c}$$

such that for all $r \in I_v^*$

$$\phi \in R_c^* \tag{13d}$$

where

$$\phi_i = \begin{cases} \phi_i^r, & i \notin I_t \\ \phi_i^r + t_i \rho_i^r, & i \in I_t \end{cases}, \qquad i \in I_\phi \tag{13e}$$

and

$$R_c^* \triangleq \{ \phi | f_i(\phi) \leq 0,\ i \in I_c^* \}. \tag{13f}$$

For the two-section transformer example, we implemented the optimization problem of (13) to find the possible tunable element(s) among $Z_1$ and $Z_2$, i.e., $I_t = \{1,2\}$. $Z_1$ was found to be the only element needed to be tunable to tune the worst-case vertices 2 and 3. Therefore, $I_t^* = \{1\}$.

As was pointed out in [1] and [2], a design centering with the identified tunable elements taken into account would result in an increase in the tolerances and thus decrease the manufacturing cost. In general, the resulting nominal design parameters after performing design centering will vary from those obtained using the minimax design optimization problem of (10).

## V. Functional Tuning Algorithms

After manufacturing and assembling, the circuit performance specifications are checked. If tuning is necessary, a sequence of tunable parameter adjustments is carried out until the specifications are met. Tuning algorithms are devised to automate the tuning assignment problem.

In practice, one of two classes of methods for postproduction tuning is employed, namely the functional tuning approach and the deterministic tuning approach [6]. In the deterministic tuning approach, all of the parameters of the manufactured circuit and the possible parasitic effects are measured. Then, a matching procedure is carried out, where it is required to match the performance functions at specified frequency points by varying the tunable parameter values. In the functional tuning approach, the actual network element values are generally assumed unknown. For example, it may be difficult to measure or identify the actual circuit element values.

In this section, two functional tuning algorithms are presented. Both algorithms are based on measuring the response of the circuit at a number of critical frequencies and formulating the postproduction tuning problem as an optimization problem.

### A. A Linear Approximation Technique for Functional Tuning

The tuning assignment problem could be formulated in a similar way to the nominal design problem, but with the tunable parameters $\boldsymbol{\rho}$ taken as the only variables [7].

Similarly to (10), the tuning assignment problem can be formulated as a minimax problem as follows:

$$\underset{\boldsymbol{\rho}, z}{\text{minimize}}\, z \tag{14a}$$

subject to

$$f_i(\boldsymbol{\phi}^0 + \boldsymbol{E}\boldsymbol{\mu}^a + \boldsymbol{T}\boldsymbol{\rho}) \leq z, \qquad i \in I_c \tag{14b}$$

$$\boldsymbol{\rho}^l \leq \boldsymbol{\rho} \leq \boldsymbol{\rho}^u. \tag{14c}$$

The superscript $a$ in (14b) refers to the actual values of a certain manufactured outcome to be tuned. $\boldsymbol{\phi}^0$, $\boldsymbol{E}$, and $\boldsymbol{T}$ are all known. $\boldsymbol{\mu}^a$ is unknown and no control could be exerted on it. The optimization is carried out by varying $\boldsymbol{\rho}$. $\boldsymbol{\rho}^l$ and $\boldsymbol{\rho}^u$ represent limits on the tuning amounts. In the case of irreversible tuning, where, for example, the elements are allowed to increase, the limits are non-negative.

Since we restrict tuning amounts by (14c), a differentiable approximation can be used to estimate the changes in the functions, and the minimax optimization problem, namely (14), can be approximated as follows:

$$\underset{\Delta\boldsymbol{\rho}, z}{\text{minimize}}\, z \tag{15a}$$

subject to

$$f_i(\boldsymbol{\phi}^0 + \boldsymbol{E}\boldsymbol{\mu}^a + \boldsymbol{T}\boldsymbol{\rho}) + \sum_{j \in I_t^*} \frac{\partial f_i}{\partial \rho_j} \Delta\rho_j \leq z, \qquad i \in I_c \tag{15b}$$

$$\rho_j^l \leq \Delta\rho_j \leq \rho_j^u, \qquad j \in I_t^*. \tag{15c}$$

Initially, $\boldsymbol{\rho}$ in (15b) is equal to $\mathbf{0}$; after each solution of the optimization problem, it is updated by $\Delta\boldsymbol{\rho}$. Optimization problem (15) is solved by a linear programing routine. The functions $f_i$ in (15b) are measured directly. The sensitivities $\partial f_i / \partial \rho_j$ should be evaluated at the actual parameter values, which are unknown. As such, we utilize a suitable approximate model $\boldsymbol{\phi}^x$ for simulating these sensitivities (a good initial value could be the nominal parameter values or the parameter values that are predicted using a least-squares estimator).

The network sensitivities could be updated using the Broyden rank-one updating formula [8] after every solution (iteration) of (15). The use of the Broyden formula, summarized in a more complete report [9], exploits the measurements in improving the initial network model $\boldsymbol{\phi}^x$. A better approximation is obtained after each iteration.

We applied this technique to tune the worst-case vertices of the two-section transformer with $\pm 20$-percent toler-

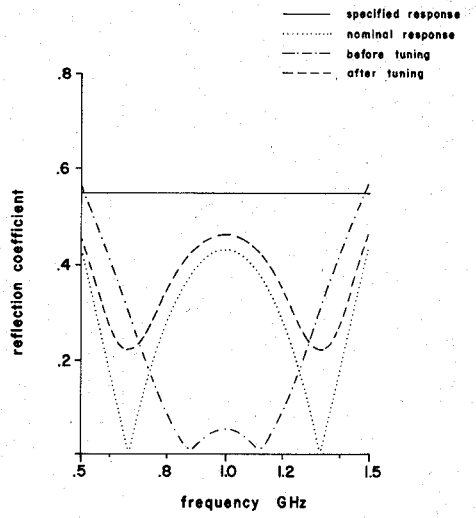


Fig. 4. The results of tuning an outcome corresponding to vertex number 3 of the two-section transformer.

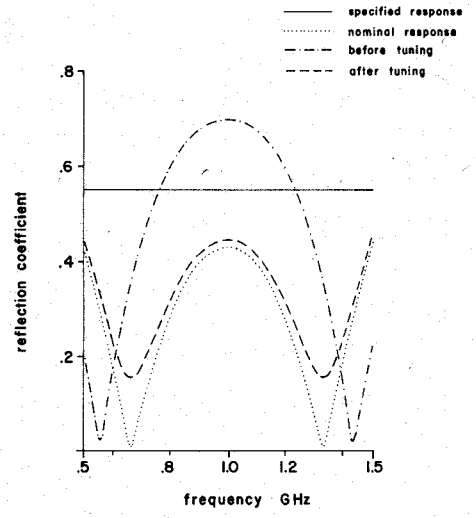


Fig. 5. The results of tuning an outcome corresponding to vertex number 2 of the two-section transformer.

ances. We stop tuning when the maximum value of the reflection coefficient over the frequency range 0.5–1.5 GHz could not be reduced further. We have taken $\rho^u_{Z_1} = -\rho^l_{Z_1} = 0.02$. Fig. 4 illustrates the responses before and after tuning for vertex number 3. Twenty-two adjustments of $Z_1$ were needed to tune the worst-case outcome. Fig. 5 illustrates the responses before and after tuning for vertex number 2. Nineteen adjustments of $Z_1$ were needed to tune the vertex. This is because we restricted $|\Delta\rho_{Z_1}|$ to be less than or equal to 0.02 and is due also to the large deviation of the response from nominal before tuning. The linear programming problem of (15) is solved using a subroutine available from the IMSL Library [10]. Note that we continued tuning even after the design specification of 0.55 is satisfied.

### B. Modeling Technique for Functional Tuning

Let $F(\phi, \omega)$ represent the response function that is monitored during the tuning process. We assume that the actual network response is given by [11]

$$F^a(\phi^a, \omega) \triangleq F^0(\phi^0, \omega) + F^d(\phi^a, \omega) \tag{16}$$

where the superscript $a$ refers to the actual values, superscript 0 refers to the nominal values, and $F^d$ gives the deviational effect due to the changes in the circuit parameters, including parasitic effects, from nominal.

We model the deviational effect by a rational transfer function in $\omega$. Let

$$F^d(\omega) = \frac{a_N\omega^N + a_{N-1}\omega^{N-1} + \cdots + a_0}{\omega^D + b_{D-1}\omega^{D-1} + \cdots + b_0} \tag{17}$$

where the degree of the numerator and that of the denominator, namely $N$ and $D$, are determined according to the characteristics of the original function $F(\phi, \omega)$, together with the different known parasitic effects that affect the performance of the network. Some of the coefficients of (17) could be set to zero as appropriate.

The coefficients of (17) are obtained from (16) since the nominal response $F^0(\phi^0, \omega_i)$ at a certain frequency $\omega_i$ is simulated, and the actual response $F^a(\phi^a, \omega_i)$ is measured directly. Measuring the response at $n_\omega$ different frequencies such that $2n_\omega > N + D + 1$, we get an overdetermined linear real system of equations in the coefficients $a_k$, $k = 0, 1, \cdots, N$ and $b_j$, $j = 0, 1, \cdots, D-1$. We solve this system of equations using the linear least-squares method to get these coefficients.

Recalling (6), the inequality constraints could be expressed as

$$\bar{f}_i(\rho) \triangleq w_i\big(F_i(\rho) + F^d(\omega_i) - S(\omega_i)\big) \leqslant 0, \qquad i \in I_c \tag{18}$$

where $F_i(\rho)$ is the response function evaluated at $\omega_i$ and

$$\phi_j = \begin{cases} \phi^0_j, & j \notin I_t^* \\ \phi^0_j + \rho_j t_j, & j \in I_t^* \end{cases}, \qquad j \in I_\phi \tag{19}$$

and where $w_i$ is an appropriate weighting function. Similarly to (10), the tuning assignment problem is formulated as follows:

$$\underset{\rho, z}{\text{minimize}}\, z \tag{20a}$$

subject to

$$z \geqslant \bar{f}_i, \qquad i \in I_c \tag{20b}$$

$$\rho^l_i \leqslant \rho_i \leqslant \rho^u_i, \qquad i \in I_t^*. \tag{20c}$$

The solution of the optimization problem (20) provides us with $\rho$. The tunable network parameters are adjusted by the amount indicated, and the process is repeated until the circuit meets its specifications.

We applied the modeling tuning algorithm to tune the worst-case vertices of the two-section transformer example. Recalling (16) and (17), we assumed that

$$F^d(\omega) = \frac{a_{10}\omega^{10} + a_8\omega^8 + a_6\omega^6 + a_4\omega^4 + a_2\omega^2 + a_0}{b_{10}\omega^{10} + b_8\omega^8 + b_6\omega^6 + b_4\omega^4 + b_2\omega^2 + b_0}$$

and the lower and upper bounds of (20c) are taken to be $\pm 0.1$. We stop tuning when the maximum value of the reflection coefficient over the frequency range 0.5–1.5 GHz could not be reduced further. The responses before and after tuning for vertex number 3 are similar to those of Fig.

4. Optimization problem (20) was performed four times. The responses before and after tuning for vertex number 2 are similar to those of Fig. 5. Optimization problem (20) was performed five times. Five iterative adjustments of $Z_1$ were carried out. Note that we have continued tuning to achieve an optimum tuned response. Also, we note the similarity between the responses after tuning, which are obtained using the linear approximation technique and the modeling technique.

### C. Tuning Algorithm

The two proposed tuning techniques could be applied on-line for the tuning of a microwave circuit as follows.

*Step 1:* Measure the network response. Check whether the design specifications are satisfied to a certain prespecified margin. If they are satisfied, stop.

*Step 2:* Utilize the performed measurements in constructing the constraint functions as well as their derivatives as required by the optimization problems (15) or (20).

*Step 3:* Solve the optimization problems (15) or (20) for the changes in the tunable parameters ($\rho$ or $\Delta\rho$). The upper and lower limits in the optimization problems are defined to ensure the validity of the approximation employed and the type of tuning.

*Step 4:* If the absolute value of a tunable element is less than the minimum amount of tuning which can be carried out in practice, we assume that it is zero. If all the absolute values of the tunable amounts are less than their corresponding minimum allowable values, stop.

*Step 5:* Adjust the parameters to the extent possible by the amounts obtained from the optimization problem. If the maximum number of iterations has not been exceeded, return to 1.

In our complete report [9], we discuss the convergence properties of the linear approximation tuning algorithm and the modeling tuning algorithm.

## VI. Example

We considered a broad-band amplifier example with a complex antenna load as shown in Fig. 6. The object is to match the antenna load over the frequency band 150–300 MHz. The power given at a certain frequency is given by

$$4R_S G_L \frac{|V_L|^2}{|V_S|^2}$$

where $R_S$ is the source resistance, $G_L$ is the real part of the admittance of the load, $|V_L|$ is the absolute value of the voltage across the load, and $|V_S|$ is the absolute value of the input voltage which we assumed to be unity. The response was assumed to be measured at sixteen uniformly distributed frequencies over the given frequency band. It is required to have a constant 10-dB power gain over the frequency band of interest. Therefore, two inequality constraints are defined at each frequency. The source resistance was assumed to be 50 Ω. The transistor scattering parameter values and the antenna impedances at the sixteen frequencies were obtained from [12].

First, we applied optimization problem (10) to get the nominal design parameters using a minimax design criterion. The nominal parameters given in [12] were used as the initial design parameters for (10). We utilized the optimization package MMLC [13] for linearly constrained minimax optimization, as described in [14]. The MMLC package is an adaptation of the MMLA1Q package [15]. In the optimization, an upper practical bound of 200 Ω was assumed for the characteristic impedances. The reoptimized nominal response is superior to that obtained in [12]. This is partly because we relaxed the bounds on the design parameters. The new and previous nominal design parameters are given in Table I. The nominal response at the sixteen chosen frequencies is listed in Table II. The re-

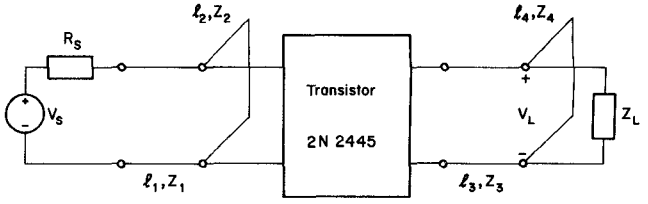


Fig. 6. The broad-band microwave amplifier.

TABLE I
NOMINAL ELEMENT VALUES AND TUNABLE AMOUNTS OF THE BROAD-BAND AMPLIFIER

| Element | Original Nominal Values | New Nominal Values | Relative Tunable Amounts |
|---|---|---|---|
| $\ell_1$ | 2 012 | 1 741 | 0 0 |
| $Z_1$ | 86 76 | 68 778 | 0 0088 |
| $\ell_2$ | 0 976 | 1 534 | 0 0 |
| $Z_2$ | 97 57 | 200 0 | 0 0 |
| $\ell_3$ | 0 833 | 1 140 | 0 0 |
| $Z_3$ | 125 | 181 252 | 0 0 |
| $\ell_4$ | 0 925 | 1 280 | 0 079 |
| $Z_4$ | 132 | 105 105 | 0 0 |

$l$ is the normalized length. The actual length equals $l\lambda_n/2\pi$, where $\lambda_n$ is the wavelength at 230 MHz. $Z$ is the characteristic impedance in ohms.

TABLE II
THE OPTIMAL NOMINAL RESPONSE AND THE WORST-CASE RESPONSE OF THE BROAD-BAND AMPLIFIER FOR ±5-PERCENT TOLERANCE

| Frequency (MHz) | Power Gain (dB) | Worst Case Vertex | Worst-Case Response (dB) |
|---|---|---|---|
| 150 | 10 058 * | 123 ** | 11 318 |
| 160 | 9 926 * | 134 ** | 8 559 |
| 170 | 10 072 * | 123 ** | 11 274 |
| 180 | 10 043 | 107 | 11 155 |
| 190 | 10 053 | 107 | 11 189 |
| 200 | 10 006 | 107 | 11 095 |
| 210 | 10 028 | 104 | 11 053 |
| 220 | 9 926 * | 153 ** | 8 794 |
| 230 | 10 031 | 104 | 10 894 |
| 240 | 10 028 | 112 | 10 765 |
| 250 | 10 072 * | 80 | 10 726 |
| 260 | 10 031 | 80 | 10 640 |
| 270 | 9 965 | 189 | 9 313 |
| 280 | 9 926 * | 189 | 9 302 |
| 290 | 9 983 | 61 | 9 392 |
| 300 | 10 072 * | 212 | 10 657 |

*identifies critical frequencies.
**identifies critical vertices. Their corresponding worst-case responses violate the specifications of ±1-dB deviation from 10 dB.

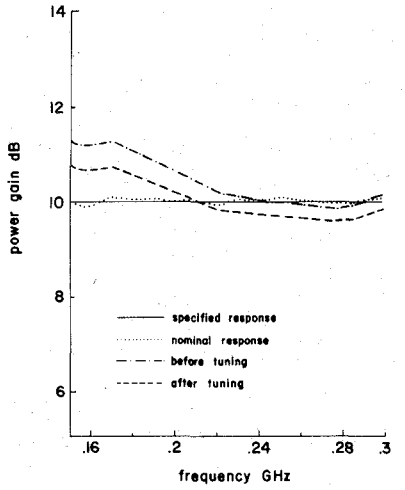


Fig. 7. The results of tuning an outcome corresponding to vertex number 123 of the broad-band amplifier using the modeling technique.

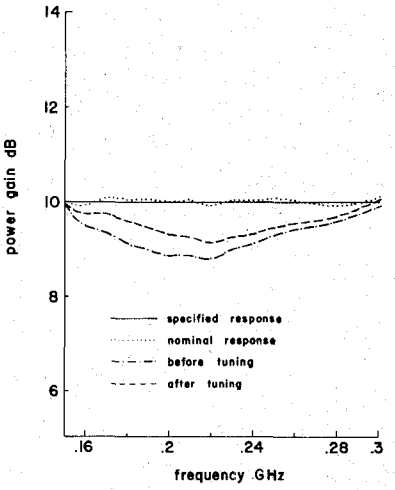


Fig. 9. The results of tuning an outcome corresponding to vertex number 153 of the broad-band amplifier using the modeling technique.

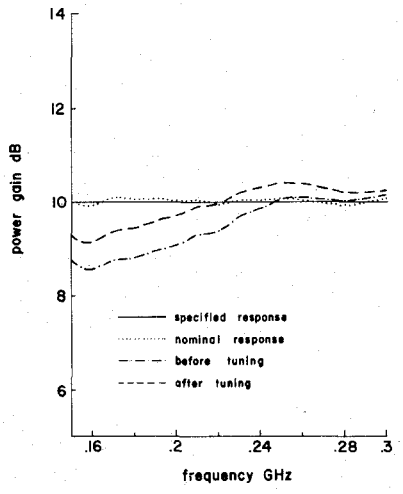


Fig. 8. The results of tuning an outcome corresponding to vertex number 134 of the broad-band amplifier using the modeling technique.

sponse alternated between maxima and minima at the critical frequency points. These frequencies, namely 150, 160, 170, 220, 250, 280, and 300 MHz, are identified by an asterisk in Table II. This set of frequencies constitutes the required $I_c^*$.

Then, a worst-case analysis is performed using $\pm 5$-percent tolerances and no parasitics are assumed. The number of vertices is equal to $2^8 = 256$. We assume that the design specifications tolerate a $\pm 1$-dB deviation from the specified value of 10 dB. At every critical frequency $i \in I_c^*$, the worst-case vertices are obtained, as well as the corresponding worst-case responses. Four worst-case responses violate the design specifications, as is shown in Table II. Consequently, the set $I_v^*$ consists of vertices $\{123, 134, 153\}$, as indicated in Table II.

Third, we performed the optimization problem (13), using the three critical vertices to determine the tunable parameters. The results of this optimization problem are given in Table I. It is clear that $Z_1$ and $l_4$ are the tunable parameters. The optimization package MFNC [16], which implements the Han–Powell algorithm described in [17], is utilized in solving this problem. The MFNC package is an adaptation of the VF02AD subroutine of the Harwell Subroutine Library [18].

TABLE III
RESULTS OF TUNING THE WORST-CASE VERTICES OF THE BROAD-BAND AMPLIFIER

| | Case 1 | Case 2 | Case 3 |
|---|---|---|---|
| Vertex No. | 123 | 134 | 153 |
| No. of Iterations of Functional Tuning Algorithm | 1 | 1 | 1 |
| Tunable Element Values | $Z_1 = 66.66$<br>$\ell_4 = 1.209$ | $Z_1 = 70.616$<br>$\ell_4 = 1.331$ | $Z_1 = 66.66$<br>$\ell_4 = 1.154$ |

Finally, we applied the modeling tuning algorithm to illustrate its utilization in tuning any possible outcome. We assumed that the actual power gain is given by

$$F^a(\omega) = F^0(\omega) + F^d(\omega)$$

where

$$F^d(\omega) = \frac{a_4\omega^4 + a_2\omega^2 + a_0}{\omega^4 + b_2\omega^2 + b_0}.$$

The lower and upper bounds in (20c) are taken to be $\pm 1$. The results of tuning for the critical vertices $I_v^*$ are given in Table III. We stop tuning when the relaxed specifications are satisfied. The lower and upper bounds of (20c) were not active at the solution and only one iteration is needed to satisfy the specifications. The responses before and after tuning are shown in Figs. 7, 8, and 9. The solution of optimization problem (20) is obtained by the optimization package MMLC [13].

## VII. Discussion and Conclusions

We have presented a unified integrated approach to the postproduction tuning problem. The approach optimally utilizes the information obtained at the design stage in

specifying both the tunable parameters and the essential tuning frequencies.

Two new functional tuning techniques are presented. The techniques optimally use available response measurements and eliminate completely the experimental trial-and-error and one-at-a-time approach. They are quite general and can be applied to any network for both reversible and irreversible tuning.

The linear approximation technique will perform quite reasonably as long as the linear approximation is valid. Carrying out the tuning procedure in stages and updating the sensitivity matrix by the Broyden formula will ensure the validity of the linear approximation.

The modeling technique usually needs fewer response measurements than the linear approximation technique, but requires much more on-line computational capabilities. For reasonably small deviations of the network elements from nominal, the technique converges in one or two iterations to the design specifications.

The techniques proposed have been implemented using well-documented computer optimization packages.

We have not emphasized design centering after identifying the tunable elements and optimally satisfying the design specifications. Such design centering would result in an increase in the tolerances and thus decrease the manufacturing cost. Optimally satisfying the design specifications would result in a better tuned response. We believe, however, that these two features are readily applicable in any practical environment, as has been already demonstrated in the literature [1]–[3].

## Acknowledgment

The authors are grateful to Dr. M. R. M. Rizk of Alexandria University, Alexandria, Egypt, for his contribution to this work in its early stages. They also acknowledge useful discussions with and the cooperation of Dr. K. Madsen of the Technical University of Denmark, Lyngby, Denmark, and W. Kellermann of McMaster University.

## References

[1] J. W. Bandler, P. C. Liu, and H. Tromp, "A nonlinear programming approach to design centering, tolerancing and tuning," *IEEE Trans. Circuits Syst.*, vol. CAS-23, pp. 155–165, 1976.

[2] J. W. Bandler, P. C. Liu, and H. Tromp, "Integrated approach to microwave design," *IEEE Trans. Microwave Theory Tech.*, vol. MTT-24, pp. 584–591, 1976.

[3] J. W. Bandler and M. R. M. Rizk, "Optimization of electrical circuits," *Mathematical Programming Study on Engineering Optimization*, vol. 11, pp. 1–64, 1979.

[4] D. E. Hocevar and T. N. Trick, "Automatic tuning algorithms for active filters," *IEEE Trans. Circuits Syst.*, vol. CAS-29, pp. 448–457, 1982.

[5] R. K. Brayton, S. W. Director, G. D. Hachtel, and L. M. Vidigal, "A new algorithm for statistical circuit design based on quasi-Newton methods and function splitting," *IEEE Trans. Circuits Syst.*, vol. CAS-26, pp. 784–794, 1979.

[6] J. W. Bandler and R. M. Biernacki, "Postproduction parameter identification and tuning of analog circuits," in *Proc. Eur. Conf. Circuit Theory and Design* (Warsaw, Poland), vol. 2, 1980, pp. 205–220.

[7] J. W. Bandler, M. R. M. Rizk, and A. E. Salama, "An iterative optimal postproduction tuning technique utilizing simulated sensitivities and response measurements," in *IEEE Int. Microwave Symp. Dig.* (Los Angeles, CA), 1981, pp. 63–65.

[8] G. C. Broyden, "A class of methods for solving nonlinear simultaneous equations," *Mathematics of Computation*, vol. 19, pp. 577–593, 1965.

[9] J. W. Bandler and A. E. Salama, "Functional approach to microwave postproduction tuning," Dept. Elec. Comput. Eng., McMaster University, Hamilton, Canada, 1984, Rep. SOS-83-29-R2.

[10] ZX3LP subroutine specification, *IMSL Library*, Houston, TX, 1982.

[11] J. W. Bandler and A. E. Salama, "Integrated approach to microwave postproduction tuning," in *IEEE Int. Microwave Symp. Dig.* (Boston, MA), 1983, pp. 415–417.

[12] E. Sanchez-Sinencio, "Computer-aided design of microwave circuits," Coordinated Science Laboratory, University of Illinois, Urbana-Champaign, IL, 1973, Rep. R-617.

[13] J. W. Bandler and W. M. Zuberek, "MMLC—A Fortran package for linearly constrained minimax optimization," Dept. Elec. Comput. Eng., McMaster University, Hamilton, Canada, 1983, Rep. SOS-82-5-U2.

[14] J. Hald and K. Madsen, "Combined LP and quasi-Newton methods for minimax optimization," *Mathematical Programming*, vol. 20, pp. 49–62, 1981.

[15] J. Hald, "MMLA1Q—A Fortran package for linearly constrained minimax optimization," Technical University of Denmark, Lyngby, Denmark, 1981.

[16] J. W. Bandler and W. M. Zuberek, "MFNC—A Fortran package for minimization with general constraints," Dept. Elec. Comput. Eng., McMaster University, Hamilton, Canada, 1983, Rep. SOS-82-6-U2.

[17] M. J. D. Powell, "A fast algorithm for nonlinearly constrained optimization calculations," *Lecture Notes in Mathematics 630*, G. A. Watson, Ed. Berlin: Springer-Verlag, 1978, pp. 144–157.

[18] VF02AD subroutine specification, *Harwell Subroutine Library*, AERE, Harwell, Oxfordshire, England, 1982.

**John W. Bandler** (S'66–M'66–SM'74–F'78) was born in Jerusalem, Palestine, on November 9, 1941. He studied at the Imperial College of Science and Technology, London, England, from 1960 to 1966. He received the B.Sc. (Eng.), Ph.D., and D.Sc. (Eng.) degrees from the University of London, London, England, in 1963, 1967, and 1976, respectively.

He joined Mullard Research Laboratories, Redhill, Surrey, England, in 1966. From 1967 to 1969, he was a Postdoctorate Fellow and Sessional Lecturer at the University of Manitoba, Winnipeg, Canada. He joined McMaster University, Hamilton, Canada, in 1969, where he is currently a Professor of Electrical and Computer Engineering. He has served as Chairman of the Department of Electrical Engineering and Dean of the Faculty of Engineering. He currently directs research, which has received substantial support from the Natural Sciences and Engineering Research Council of Canada under its Operating and Strategic Grants Awards, in the Simulation Optimization Systems Research Laboratory.

He is also currently President of Optimization Systems Associates. He has provided consulting services and software to numerous organizations in the electronic, microwave, and electrical-power industry, specializing in advanced applications of simulation, sensitivity analysis, and mathematical optimization techniques.

He is a contributor to *Modern Filter Theory and Design*, Wiley-Interscience, 1973. He has over 190 publications, four of which appear in *Computer-Aided Filter Design*, IEEE Press, 1973, one in *Microwave Integrated Circuits*, Artech House, 1975, and one in *Low-Noise Microwave Transistors and Amplifiers*, IEEE Press, 1981. Dr. Bandler was an Associate Editor of the IEEE TRANSACTIONS ON MICROWAVE THEORY AND TECHNIQUES (1969–1974). He was Guest Editor of the Special Issue of the IEEE TRANSACTIONS ON MICROWAVE THEORY AND TECHNIQUES on Computer-Oriented Microwave Practices (March 1974).

Dr. Bandler is a Fellow of the Institution of Electrical Engineers (Great Britain) and a member of the Association of Professional Engineers of the Province of Ontario (Canada).

**Aly E. Salama** (S'79–M'83) was born in Cairo, Egypt, on June 8, 1954. He received the B.Sc. and M.Sc. degrees, both in electrical engineering from Cairo University, Egypt, in 1975 and 1979, respectively, and the Ph.D. degree from McMaster University, Hamilton, Ontario, Canada, in 1983.

From 1975 to 1979, he worked as a Teaching and Research Assistant in the Department of Electronics and Electrical Communications Engineering, Cairo University. From 1979 to 1983, he was a Teaching and Research Assistant in the Department of Electrical and Computer Engineering, McMaster University. From July 1983 to July 1984, he worked as a Postdoctoral Fellow in the Department of Electrical and Computer Engineering, McMaster University, under the supervision of Dr. J. W. Bandler. He is currently an Assistant Professor in the Department of Electronics and Electrical Communications Engineering, Cairo University, Egypt. His research interests include all aspects of computer-aided design with emphasis on fault location and parameter tuning.

# Short Papers

## Highly Stable Dielectric Resonator FET Oscillators

CHRISTOS TSIRONIS, MEMBER, IEEE

*Abstract*—**The long-term frequency drift of GaAs FET oscillators with temperature has been analyzed theoretically and experimentally in view of stabilization using dielectric resonators. It was found that the dielectric material stability and quality factor should be within certain limits, and, in addition, that the resonance frequency over the temperature characteristic should be quite linear. Such a material has been developed on the basis of $BaTi_4O_9$ and $Ba_2Ti_9O_{20}$, and ultra-stable DRO's with frequency drifts of around ± 100 kHz for −50 to 100°C at 11 GHz ( ≈ ±0.06 ppm/K) have been realized.**

### I. Introduction

Dielectric resonator stabilized oscillators (DRO's) are simple, small-sized, and consequently low-priced subassemblies the performances of which (concerning frequency stability, reliability, compactness, and electrical efficiency) have reached a level sufficient for several professional applications [1]. In work hitherto done on the stabilization of DRO's [2]–[4], it has, in fact, been recognized that the temperature properties of the active oscillator part, comprising the FET (or Gunn-diode) and the associated circuitry, are important for the stabilization mechanism, but an explicit investigation on this phenomenon has first been reported by the author in 1982 [5]. Similar to the work of Komatsu *et al.* [4], a stacked-type resonator with a temperature coefficient $\tau_f$ ( $= df_r/f_r dT$) constant over temperature has been reported in [5] and been used to realize highly stable DRO's. However, the stacked-type resonator does not represent an industrial solution. A new material performing the desired stability $\tau_f$, linearity ($d\tau_f/dT \rightarrow 0$), and quality factor $Q_r$, as defined in [5], in view of frequency stability, but also of the power degradation with temperature, had to be developed. This work has been done successfully at Philips Research Laboratories in Aachen, West Germany. This paper deals with the temperature behavior of FET DRO's using this new material, which allows even better results than achieved with the stacked-type resonator as reported before [4], [5].

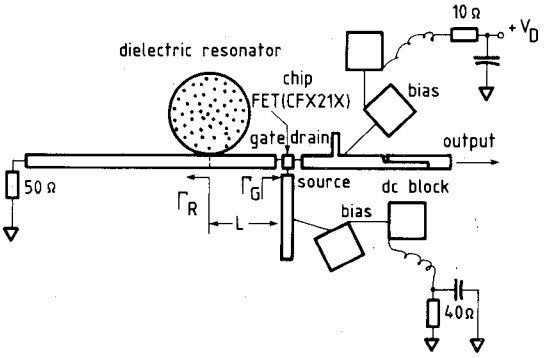


Fig. 1. Microstrip layout of GaAs FET DRO used in this work. $\Gamma_R$ and $\Gamma_G$ indicate the resonator and active circuit reflexion coefficients used in temperature modeling [5].

### II. Modeling of Long-Term Frequency Stability

In this context, only the main results of the theoretical analysis presented in [5] on the temperature stabilization procedure of GaAs FET reflexion-type DRO's (Fig. 1) will be used. They can be summarized in the stabilization formula (1) and the temperature-stability-power-coupling chart of Fig. 3. This chart serves to demonstrate the stabilization limits for different resonator materials taking into account the oscillation power.

Manuscript received June 12, 1984; revised November 5, 1984.

The author is with Laboratoires d'Electronique et de Physique Appliquée, 3 Avenue Descartes, 94450 Limeil-Brevannes, France.

0018-9480/85/0400-0310$01.00 ©1985 IEEE